

## Estimation of fluid loading on offshore structures

N. HOGBEN, B. L. MILLER, J. W. SEARLE & G. WARD

**Dr D. J. Maull**, University Engineering Department, Cambridge

The Authors state that using values of  $C_D$  and  $C_M$ , which are functions of the Keulegan-Carpenter number, to calculate the forces on circular cylinders in waves results in good agreement with experiment except near Keulegan-Carpenter numbers of 10-15. However, for some applications it may be necessary to consider  $C_D$  and  $C_M$  not as variables but as constants. For instance, Fig. 9 shows the root mean square force  $F$  on a circular cylinder of diameter  $D$  in a unidirectional sinusoidal flow generated in a U tube, the force being in the direction of the flow.  $T$  is the periodic time of the motion and  $N_K$  the Keulegan-Carpenter number. The root mean square force given by Morison's equation

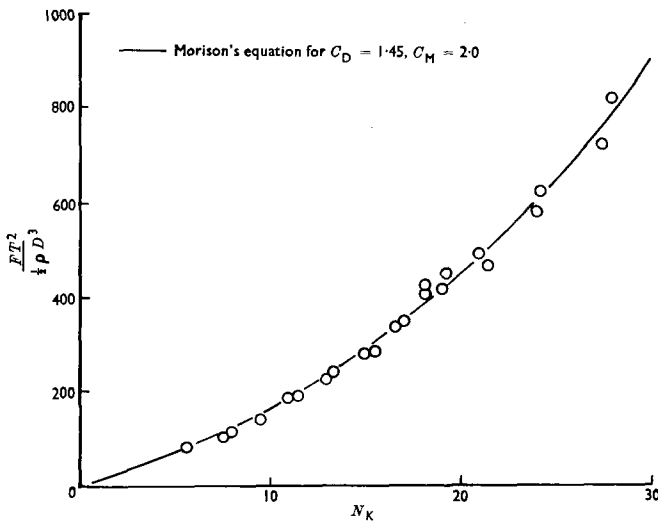


Fig. 9. Root mean square drag force versus Keulegan-Carpenter number

## DISCUSSION

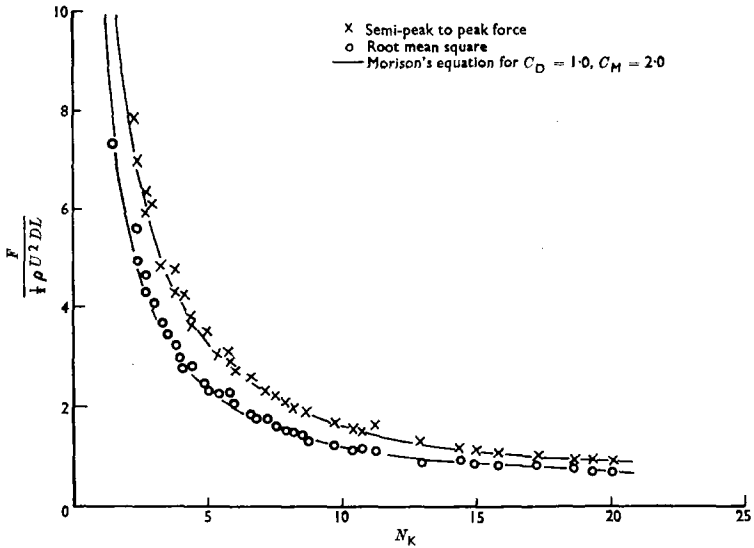


Fig. 10. Vertical cylinder in waves

with constant values of  $C_D$  and  $C_M$  gives good agreement with experiment over a wide range of  $N_K$ .

122. The root mean square and semi-peak to peak force on a vertical cylinder in waves are also well predicted by Morison's equation using constant values of  $C_D$  and  $C_M$  as shown in Fig. 10 which is taken from Isaacson.<sup>121</sup> In both Figs 9 and 10 the value of  $C_M$  taken is 2.0—the value given by potential flow theory.

123. The Authors mention that lift forces may also be generated due to vortex shedding, but it must be pointed out that the results published may exhibit considerable scatter. For instance, Fig. 11 shows the root mean square lift force  $L$  measured on a circular cylinder in a U tube,  $L$  being normal to the flow direction. Over some ranges of  $N_K$  there is considerable scatter of the results and analysis of the force traces shows that this is caused by intermittent vortex shedding. This flow is analysed in reference 122.

124. Horizontal cylinders under waves have been investigated<sup>123</sup> and results show that an application of the Morison equation, using conventional values of  $C_D$  and  $C_M$ , overestimates the forces on the cylinder in the wave propagation direction. However, substantial lift forces can be generated due to the vortex shedding being altered by the vertical component of velocity under the waves.

125. All the results mentioned were obtained at Cambridge University under laboratory conditions and are at low subcritical Reynolds numbers.

**Mr R. Burrows, Dr J. R. Chaplin, Mr T. S. Hedges, Professor P. Holmes and Mr R. G. Tickell,** Department of Civil Engineering, University of Liverpool

In their original work Morison *et al.*<sup>1</sup> were concerned only with the ocean wave loading on vertical cylindrical members, for which the total load per unit length was assumed to be horizontal and was expressed in the form of equation (2). However, as stated in the Paper, little attention has been given to the loading mechanism resulting from wave-induced fluid motion around non-vertical members, although some writers have

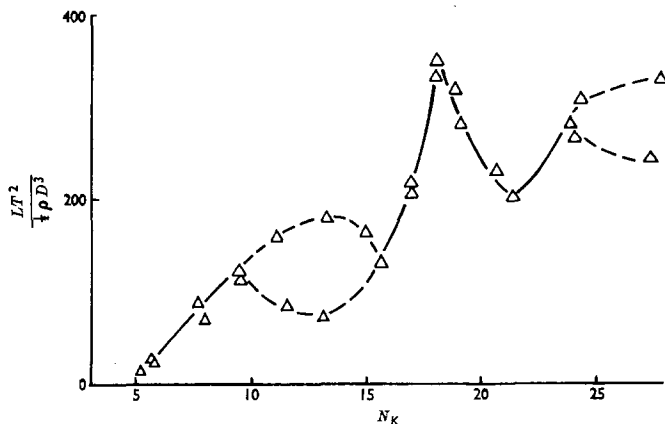


Fig. 11. Root mean square lift force on a circular cylinder in sinusoidal flow versus Keulegan-Carpenter number

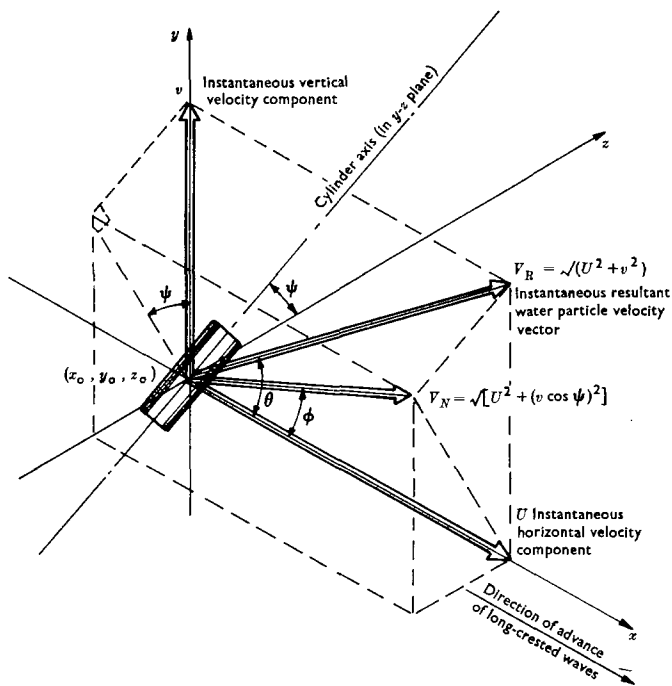


Fig. 12

## DISCUSSION

assumed that the load in any particular direction may be derived by using only the components of the water-particle motions in that direction.<sup>124-126</sup> Indeed this assumption appears to have been made in the Author's general statement of Morison's equation (equation (1)).

127. We developed a more thorough representation of the loading mechanism for inclined members lying in a plane parallel to the wave crests for application to a North Sea production platform. This representation follows the cross-flow principle outlined in § 53 and is in agreement with the work of Borgman<sup>127</sup> on members of arbitrary orientation with respect to the waves.

128. Consider a unit length section of cylindrical member submerged beneath the water surface at location  $(x_0, y_0, z_0)$ , as shown in (Fig. 12). The  $x$ - $z$  plane is horizontal and the member is inclined at an angle  $\psi$  to the  $z$  axis in the  $y$ - $z$  plane. Regular long-crested waves are assumed to advance in the positive  $x$  direction.

129. At a particular instant the resultant velocity vector at location  $(x_0, y_0, z_0)$  will be inclined at an angle  $\theta$  to the horizontal, where  $\theta$  varies between 0 and  $2\pi$  during the passage of each wave. Furthermore, the resultant velocity vector, giving rise to the drag component of loading, is out of phase with the resultant acceleration vector, giving rise to the inertial component of loading, and thus the total force at any instant must be evaluated using vector addition of these two components.

130. In the supercritical and post-critical flow regimes the contribution of skin friction to the total drag will be negligible and the total force may then be assumed to be determined essentially by the pressure difference across the cylinder. Consequently, it acts normal to the member axis in the direction of  $V_N$  (the normal component of the resultant water particle velocity  $V_R$ ) and may be written as

$$F_{DN} = \frac{1}{2}\rho C_D D [U^2 + (v \cos \psi)^2] \quad . . . . . (17)$$

131. The drag components in the co-ordinate directions are

$$\left. \begin{aligned} F_{Dx} &= F_{DN} \cos \phi = \frac{1}{2}\rho C_D D U \sqrt{[U^2 + (v \cos \psi)^2]} \\ F_{Dy} &= F_{DN} \sin \phi \cos \psi = \frac{1}{2}\rho C_D D v \sqrt{[U^2 + (v \cos \psi)^2]} \cos^2 \psi \\ F_{Dz} &= -F_{DN} \sin \phi \sin \psi = -F_{Dy} \tan \psi \end{aligned} \right\} . . . (18)$$

132. The inertia loading may be estimated in a similar way if it is assumed that only accelerations in a plane normal to the member axis are significant,<sup>128</sup> yielding

$$F_{IN} = \rho \frac{\pi D^2}{4} C_M \left[ \left( \frac{dU}{dt} \right)^2 + \left( \frac{dv}{dt} \cos \psi \right)^2 \right]^{1/2} . . . . . (19)$$

133. Reducing this force to its components in the co-ordinate directions and adding the appropriate drag force gives the components of the total force as

$$\left. \begin{aligned} F_x &= \frac{1}{2}\rho C_D D U \sqrt{[U^2 + (v \cos \psi)^2]} + \rho \frac{\pi D^2}{4} C_M \frac{dU}{dt} \\ F_y &= \left[ \frac{1}{2}\rho C_D D v \sqrt{[U^2 + (v \cos \psi)^2]} + \rho \frac{\pi D^2}{4} C_M \frac{dv}{dt} \right] \cos^2 \psi \\ F_z &= -F_y \tan \psi \end{aligned} \right\} . . . (20)$$

134. For a vertical member  $\psi = 90^\circ$  and  $F_x$  simplifies to equation (2) with  $F_y = F_z = 0$ . In this special case of the general condition the vertical member is still subject to the application of the cross-flow principle because the resultant water particle velocity vector is rotating in a vertical plane normal to the wave fronts and, therefore, is perpendicular to the member axis under wave crests and troughs only.

135. In contrast, a horizontal member with its axis parallel to the wave crests represents a condition in which the resultant rotating velocity vector is always perpendicular to the member axis, obviating the need to apply the cross-flow principle. For such a member  $\psi = 0$  and  $F_x$  simplifies to<sup>129</sup>

$$F = \frac{1}{2}\rho C_D D U \sqrt{[U^2 + v^2]} + \rho \frac{\pi D^2}{4} C_M \frac{dU}{dt} . . . . . (21)$$

A similar expression exists for the vertical loading, but with the roles of  $U$  and  $v$  reversed. In this situation  $F_z$  is zero.

136. The form of the drag component in equation (21) leads us to query the statement in § 43 regarding the choice of  $C_M$  and  $C_D$  for horizontal members. Although the values of  $C_M$  may be the same, clearly a larger value of  $C_D$  is required in equation (2) than is necessary in equation (21) if the same force is to be predicted. Consequently, there is a need to specify which form of the loading expression for horizontal members is to be used in conjunction with the coefficient values in Fig. 1. Equation (1) suggests one form but application of the cross-flow principle outlined in § 53 suggests another—equation (21).

137. In § 58 the Authors comment on the effects of the proximity of the sea bed on the forces on pipelines. Presumably similar effects, involving modifications to the vortex shedding pattern and wake size, also occur for horizontal members just beneath the water surface, although in this case there will be the added complication of surface waves being generated. Such conditions can exist, for example, during platform tow-out operations. Proximity effects at the sea bed and at the surface are in some ways similar to those for neighbouring cylinders spaced normal to the flow (§§ 49 and 51). Thus, proximity effects may only need to be considered when cylinders are within about two diameters of the boundaries.

138. For predicting loads resulting from wave slamming, it is assumed in § 63 that the significant velocity of impact is that of the wave profile itself, rather as if the water were travelling as a solid body. On this basis it follows that, except for very steep waves, slamming is predominantly a vertical force. However, the results of experiments carried out at Liverpool University<sup>130</sup> suggest that horizontal and vertical components of slam may be of the same order of magnitude for all wave steepnesses, depending on the elevation of the cylinder relative to mean water level.

139. As a concept of the slamming mechanism, it is surely reasonable to consider the impact as one with the water particles which lie in the free surface, but have velocity components different from those of the profile itself. The direction in which the induced load acts would then be that of the local particle velocity vector, which is vertical only if the impact occurs at a point on the profile near mean water level.

140. Experimental results presented by Holmes *et al.*<sup>130</sup> are compatible with this concept and therefore suggest that the slamming force per unit length should be written as

$$F_s = \frac{1}{2} \rho C_s D V_R^2 \quad \dots \dots \dots (22)$$

and that its direction is that of the local particle velocity vector, magnitude  $V_R$ .

141. Slamming coefficients evaluated on this basis were found to be in the range 0.7–2.9. Using equation (3) Miller<sup>118</sup> found the range 2.6–4.6.

142. In § 67 it is concluded that in deep water conditions predictions of loading using linear wave theory are very close to those using Stokes' fifth order theory. While calculated particle velocities and accelerations may be similar, other wave characteristics, such as celerity and free surface profile, may differ markedly between the two theories. The free surface profile is especially important in calculations of slamming loads.

143. When taken to sufficiently high order, the stream function wave theory provides a better fit to the surface boundary conditions over the whole range of engineering interest than any other available theory.<sup>131</sup> We therefore strongly recommend its use for all design wave calculations, except those which for other reasons rely on linear wave theory, and possibly those which may be carried out entirely by hand for small amplitude waves.

144. It is misleading to suggest (§ 68) that the stream function theory may be used to analyse irregular waves without noting that in order to do so it is necessary to assume that the free surface profile is travelling without change of form at constant celerity. The problem is then over-specified and in general no exact solution exists.

## DISCUSSION

145. Attention should be drawn to the comments in §40 regarding the essential difference in approach between assuming deterministic models for fluid flow and the inherently random nature of the flow induced by storm waves. For example, the basis on which to estimate equivalent values of  $R_e$  and  $N_K$  is obscure and this would make it difficult for the designer to use Figs 1 and 3. Furthermore, the potential importance of the directional distribution of energy in short-crested random seas is hidden in the analysis of the wave force data by the use of deterministic wave theories. This latter problem is relevant to the estimation or interpretation of both in-line and transverse force components. We consider that these questions could be particularly important in assessing the fatigue strength of platforms.

**Professor T. Sarpkaya**, Naval Postgraduate School, Monterey, California

Throughout the Paper the Authors emphasize the need for caution in applying either steady flow or planar oscillatory flow results to waves and the fact that there are other effects in the real sea situation, such as orbital motion of the fluid particles and irregularity of the sea waves, which are not taken into account by the Reynolds number and the Keulegan-Carpenter number. They also point out that 'In assessing the significance of results from experiments in planar oscillatory flow it is important to appreciate that, despite the agreement with post-critical steady flow and some wave experiments, rectilinear oscillatory motion does not model completely the orbital motion or the directional and spectral properties of the flow in sea waves experienced by offshore structures' (§40). In view of this, the Authors' logic in defence of their suggested values (Fig. 1) appears to be inconsistent.

147. The experiments of Keulegan and Carpenter,<sup>3</sup> Rance<sup>28</sup> and myself<sup>31, 48</sup> were all conducted with simple harmonic motion (and the vertical component of velocity in Keulegan and Carpenter's experiments in a small vessel never exceeded 5% of the horizontal component of velocity). Rance assumed  $C_M=2$  and did not determine it from experiments as Table 1 implies. None of the evaluators of the data for the Gulf of Mexico wave force projects I and II took into consideration the effect of currents. The NMI work on rough cylinders<sup>41</sup> did not report any drag or inertia coefficient—only the ratio of the total force acting on a smooth and a rough cylinder for relatively small Keulegan-Carpenter and Reynolds numbers. The agreement between the estimated mean values of the drag coefficient with that obtained in reference 48 clearly shows that the sectional drag coefficient could have been much higher and closer to that obtained by Sarpkaya at higher Reynolds numbers.

148. In spite of this, the Authors recommended use of Keulegan-Carpenter data for the wave force normal to the axis of a smooth cylinder in the subcritical region ( $R_e$  less than about  $10^5$ ). (In references 31 and 48 I showed that Keulegan-Carpenter data cannot be applied to Reynolds numbers larger than about 25 000.) The Authors also recommend (§33) that the drag coefficient within the subcritical regime should be reduced from 1.2 to 0.6 as the Reynolds number increases from about  $5 \times 10^4$  to  $5 \times 10^5$ . In the supercritical and postcritical regimes, they recommended a drag coefficient of 0.6. Is it not true that the two recommendations exactly add up to the drag coefficient data I presented for smooth cylinders for Reynolds numbers of from about  $10^4$  to  $1.5 \times 10^6$ ? In spite of their cautionary remarks, the Authors end up defending their recommendations with the results of carefully conducted laboratory experiments with harmonic flows and with steady flows.

149. Notwithstanding the objections to idealized experiments and the inconsistency between the recommendations and cautionary remarks of the Authors, it is recommended that the designers of offshore structures use

- (a) the drag and inertia coefficients presented in reference 31 for smooth cylinders for Reynolds numbers of from about  $10^4$  to  $10^6$ , with a constant value of  $C_D=0.62$  for higher Reynolds numbers and an inertia coefficient of  $C_M=1.8$

- (b) a drag coefficient of  $C_D=1.4$  and an inertia coefficient of  $C_M=1.5$  for marine roughened cylinders with proper allowance for the effective diameter of the cylinder.

It is also recommended that the total force be calculated by integrating the sectional force along the pile. The drag and inertia coefficients appropriate to the prevailing local Keulegan-Carpenter and Reynolds numbers should be used. The effect of orbital motion is negligible for Keulegan-Carpenter numbers larger than about 30.

### Dr Hogben, Dr Miller, Dr Searle and Dr Ward

In preparing our reply to the discussion we have noticed several errors and omissions, mainly in Appendix 2. The amended Appendix 2 and the associated tables are given on pages 963–965. Also the left-hand side of equation (15) should read  $k_0 + 1$ .

151. Dr Maull's comment that we rate  $C_D$  and  $C_M$  values as reliable except when  $N_K=10$  or 15 is a misrepresentation. Fig. 1 shows that we only suggest this for the subcritical regime of Reynolds number which has limited interest in the present context of loading on offshore structures. At higher Reynolds numbers of more practical importance for most full-scale structures, reliability at least in the drag dominated range of  $N_K$  is generally rather poor. This point, which is emphasized in the Paper, must be borne in mind in assessing the significance of Dr Maull's work because the experiments were all confined to the subcritical regime of Reynolds number.

152. The key point about Figs 9 and 10 is that they plot root mean square and semi-peak to peak forces which are unaffected by changes of phase of the force record which would cause corresponding changes in  $C_D$  and  $C_M$  as defined by conventional analysis methods. Dr Maull finds that he can in this way fit his results using constant values of  $C_D$  and  $C_M$ . The inference is that much of the variability in the coefficients reported in the literature may be due merely to changes in the phase of the force. This is a significant idea but more needs to be known about its interpretation and particularly its validity at higher Reynolds numbers before its practical implications in the context of offshore structures can be assessed.

153. Some recent experiments at the NMI used an oscillating cylinder, which will provide an opportunity to explore the validity of Dr Maull's ideas at higher Reynolds numbers ( $R_0$  up to about  $3 \times 10^5$  at  $N_K$  down to about 18 achieved by a cylinder of diameter 25 cm oscillated with a stroke up to 1.5 m at periods down to about 4 s in calm water, waves and simulated current). Reference may also be made to the major large-scale experiments in the sea at Christchurch Bay,<sup>12</sup> which should shed further light on the higher Reynolds number regime.

154. Dr Maull also notes that root mean square values of the lift force, unlike those of the in-line force, display a wide scatter at some  $N_K$  (especially  $N_K=10-15$ ) as shown in Fig. 11. He attributes this to intermittent vortex shedding and draws attention to the way in which it can be modified by the vertical component of velocity in the case of a horizontal cylinder in a wave.

155. The comments by Mr Burrows and his colleagues raise some interesting points. We agree with the analysis which results in the drag component being proportional to  $U^2 + (v \cos \psi)^2$ . Equation (1) should have referred to velocity without reference to a particular direction, as was done in reference 3, with equation (2) then applying to the particular case of a horizontal force on vertical, surface-piercing circular cylinders. The extra velocity term indicated in the contribution by the Liverpool team should be considered when calculating forces on inclined cylinders. However, the comment in §43—that the  $C_D$  and  $C_M$  values shown in Fig. 1 should be considered applicable to horizontal cylinders in the absence of data specific to horizontal cylinders—still applies. Forces on horizontal cylinders are local, in terms of depth, and in practical situations, where  $R_0 > 5 \times 10^5$ . Fig. 1 indicates that such calculations can be in error by more than 50%, which perhaps puts the matter in perspective.

## DISCUSSION

156. The Liverpool team suggest that similar effects to those experienced by pipe-lines near the sea bed also are experienced by members close to the surface. We would agree, but it would seem that for the latter the situation is more complex. Perhaps this is a topic for further research.

157. There have been some recent developments in our views on slamming resulting from discussions with Dr J. Wellicome and the staff of the Wolfson Marine Craft Unit (WMCU) at Southampton University. The significance of the experimental and theoretical results in relation to design have not yet been properly evaluated—this evaluation is part of further projects by the NMI and the WMCU, funded by the Department of Energy—but so far it has been found that

- (a) the distortion of the water surface on impact must be accounted for in theoretical models of slamming; when this is done a theoretical value of  $2\pi$  is obtained for the slamming coefficient of a circular cylinder
- (b) there are significant rise times in slamming force application due to oblique impact of cylinder and water surfaces
- (c) decay times of the slamming force are much shorter than predicted by any of the theoretical models; this is particularly important when evaluating the dynamic response of structural elements.

158. It appears that the coefficients observed in the NMI experiments are consistent with the theoretical value of  $2\pi$  when one uses realistic rise and decay times. Further details are given in the discussion of reference 118. The expected values of slamming coefficient in directional seas (where the coefficients incorporate the structural response of the member and are applied in essentially static loading calculations ignoring dynamic response) are probably in the range 3–4, in agreement with those reported by Webb.<sup>132</sup>

159. The velocity of impact was not assumed to be that of the wave profile but that of the water surface normal to itself. This is the component of water particle velocity normal to the surface at the instant of impact. In our experiments we could not detect significant differences between the direction of the slamming force and the normal to the water surface. For the experimental force traces presented in reference 11 the comparisons between estimated surface inclination (using linear wave theory which cannot be expected to be particularly accurate for the waves involved) and slamming force direction are given in Table 9.

160. Tangential components of slamming do exist (seaplane landing is an extreme example) and may be of comparable magnitude to the normal component either when the normal component has decayed considerably or when the member is near the wave trough or crest (non-breaking waves only). In general, however, tangential components may be ignored when slamming forces are large. Consequently we do not agree that the direction of the slamming force should be taken as that of the particle velocity vector.

161. On the question of wave theory selection and its significance in relation to slamming, if the important velocities were the resultant particle velocities as suggested in §§ 138–140 the same arguments would apply to both slamming and conventional

Table 9

Direction of normal to surface (measured from vertical)	Slamming force direction (measured from vertical)
8°	0°
16°	16°
8°	9°
15°	9°

wave loading. However, because the normal velocity component usually governs the slamming load the inclination of the surface at impact is important, particularly for steep waves. The significance of wave theory is to be examined in the current NMI project. On wave theories in general we take the view that, provided any integrations are carried out up to the local surface elevation, linear theory is often adequate for wave loading estimation in deep water.

162. On the selection of  $C_M$  and  $C_D$  and the estimation of equivalent  $R_o$  and  $N_K$  values in the context of random loading calculations, we would comment that in practice one is usually only concerned with the post-critical  $R_o$  regime. This does not, however, remove the problem of deciding on the value of  $N_K$  appropriate to random loading. Marshall<sup>133</sup> discusses the influence of directional seas on fatigue life calculation.

163. On fatigue in general, we think it is as well to bear in mind the limitations of the cumulative damage model (i.e. the Palmgren–Miner rule and stress cycle counting methods) and the uncertainties in fatigue properties of welded structures in corrosive media when choosing loading coefficients. These uncertainties of material behaviour appear to be at least an order of magnitude greater than long-term average uncertainties in the loading coefficients.

164. Professor Sarpkaya has raised several points illustrating the difficulties involved in giving guidance to designers in a situation of considerable uncertainty. Broadly the problems are as follows.

- (a) Low Reynolds number experiments in waves and plane oscillatory flow appear to be in reasonable agreement. The repeatability and reliability of the latter tests, exemplified by Professor Sarpkaya's studies, are much higher than any known wave experiments.
- (b) At high Reynolds numbers the results from tests in planar/oscillatory flow and steady flow are also in agreement for smooth cylinders. One can argue that flows at very high  $N_K$  values are effectively the same as steady flow. This is not contradicted by the above results.
- (c) For roughened cylinders there is only one known large-scale experiment (attributed to Blumberg and cited by Wong<sup>134</sup>) where a  $C_D$  value of 1 was quoted. This is an approximate agreement with steady flow results but not with planar oscillatory flow. Further NMI experimental work in waves has yet to be analysed in detail. We have chosen to apply the argument that the flow in waves asymptotically approaches steady flow (as far as the cylinder is concerned) as the Keulegan–Carpenter number increases. We have therefore recommended the use of steady flow values. However, there is a problem in deciding when (i.e. at what  $N_K$  value) such an approach constitutes an adequate approximation.

165. We therefore agree that Professor Sarpkaya's results may be applied up to Reynolds numbers of around  $10^6$  for smooth cylinders as implied in our citation of references 30 and 31 in Fig. 1. Also, within admittedly inadequately defined restrictions, we would agree that his results for both smooth and rough cylinders may be used for wave flows at post-critical Reynolds numbers (the practically important regime). These tentative restrictions are

- (a) when the flow is similar to planar flow (in very shallow water waves) for both horizontal and vertical cylinders
- (b) when the cylinder motion within waves causes the flow to approach planar flow (e.g. marine risers oscillating with large amplitude in comparison with local particle motions)
- (c) for vertical cylinders, below some threshold  $N_K$  value as yet unknown.

For horizontal cylinders the situation is even more uncertain.

166. We have therefore made the recommendations given in Fig. 1 having considered all the evidence available to us, accepting the limitations of the analysis of

## DISCUSSION

previous full-scale data, and have tried to indicate the uncertainties and errors which can occur.

167. We suggest that, where there are grounds for expecting planar flow results to apply (within restrictions (a) and (b) in § 165), the designer uses the values presented by Professor Sarpkaya. We do not, however, feel that we can alter our recommendations for the more general case. When the results of further laboratory and full-scale experiments are available the situation must be reappraised.

168. It seems possible that some upward revision of  $C_D$  values may be needed, especially for rough cylinders over a restricted range of  $N_K$  values. However, it does not automatically follow that these will lead to significant increases in calculated loads because increases in  $C_D$  can be accompanied by reductions in the inertia coefficient  $C_M$ . Thus where the loading comprises comparable contributions from drag and inertia, the gain in drag may be offset by a reduction in the inertia loads.

169. Important new data are now becoming available from the large-scale real environment experiments by the NMI in Christchurch Bay;<sup>12</sup> Bishop and Holmes<sup>135</sup> have presented some preliminary results.

170. Clearly there are differences of opinion in some areas which will be resolved only by further, especially large-scale, research.

## References

121. ISAACSON M. DE ST. Q. *The forces on circular cylinders in waves*. PhD thesis, Cambridge University, 1974.
122. MAULL D. J. and MILLINER M. Sinusoidal flow past circular cylinders. Submitted for publication.
123. NORMAN S. G. *The forces on horizontal circular cylinders under waves*. PhD thesis, Cambridge University, 1977.
124. MALHOTRA A. K. and PENZIEN J. Nondeterministic analysis of offshore structures. *J. Engng Mech. Div. Am. Soc. Civ. Engrs*, 1970, **96**, EM6, Dec., 985-1003.
125. MILGRAM J. H. Waves and wave forces. *Proceedings of the Conference on the behaviour of offshore structures, Trondheim*. Norwegian Institute of Technology, 1976, 11-38.
126. AL-KAZILY M. F. *Forces on submerged pipelines induced by water waves*. Hydraulic Engineering Laboratory, University of California, 1972.
127. BORGMAN L. E. Computation of the ocean-wave forces on inclined cylinders. *Trans. Am. Geophys. Un.*, 1958, **39**, No. 5, 885-888.
128. DET NORSKE VERITAS. *Rules for design, construction and inspection of fixed offshore structures*. Det Norske Veritas, Oslo, 1974.
129. HOLMES P. *et al.* *Prediction of long-term wave loading on offshore structures*. University of Liverpool, 1975, Report on Section A of Offshore Structures Fluid Loading Advisory Group Project 5.
130. HOLMES P. *et al.* *Wave slamming loads on horizontal members*. University of Liverpool, 1977, Report on Offshore Structures Fluid Loading Advisory Group Project 2.
131. DEAN R. G. *Evaluation and development of water wave theories for engineering application*. US Army, Corps of Engineers, Coastal Engineering Research Center, 1974, Special report 1.
132. WEBB R. M. Discussion on Research into environmental loading of offshore structures. Society of Underwater Technology, London, Lunch-time meeting on 31 March 1977. *To be published*.
133. MARSHALL P. W. Preliminary dynamic and fatigue analysis using directional spectra. *J. Petrol. Technol.*, 1977, **29**, June, 715-722.
135. BISHOP J. R. and HOLMES P. Design of the UK Christchurch Bay wave force project and some initial results. *Proc. EUROPEC Conference, London, 1978*, Paper 13.

134. WONG F. Y. F. Preliminary survey of the drag coefficient of circular cylinders. Lloyds Register of Shipping, London, 1973. *Unpublished.*

## Appendix 2. Assessment of the significance of errors in the wave force coefficient values on the evaluation of the wave force

110. Tables 5–8 are based on linear wave theory and apply to circular cylinders. They may be used to assess the significance of any errors in the wave force coefficient values on the evaluation of the wave force.

111. The relative magnitude of the drag force  $F_D$  to the inertia force  $F_I$  at the instant of maximum wave force at a particular depth is given by

$$\begin{aligned} F_D/F_I &= 2\Phi^2 - \frac{1}{2} & \text{for } \Phi > \frac{1}{2} \\ F_D/F_I &= 0 & \text{for } \Phi < \frac{1}{2} \end{aligned}$$

where

$$\Phi = \frac{C_D N_K}{C_M \pi^2}$$

112. Table 5 gives values of  $F_D/F_I$  as a function of the ratio  $C_D/C_M$  and  $N_K$ .

113. The relative magnitude of the maximum drag force  $F_{D \max}$  to the maximum inertia force  $F_{I \max}$  occurring during a wave cycle at a particular depth is given by

$$\frac{F_{D \max}}{F_{I \max}} = \frac{C_D N_K}{C_M \pi^2} = \Phi$$

114. Table 6 gives values of  $F_{D \max}/F_{I \max}$  as a function of the ratio  $C_D/C_M$  and  $N_K$ . At the instant of maximum force and when  $\Phi > \frac{1}{2}$

$$\left(\frac{F_{D \max}}{F_{I \max}}\right)^2 = \frac{1}{2} \left(\frac{F_D}{F_I}\right) + \frac{1}{4}$$

115. The maximum allowable error in  $C_M$  in drag dominant conditions for less than 10% relative error in the maximum force at a particular depth may be estimated as follows.

116. Take the error in  $C_M$  as  $\alpha$ , such that  $C_M = C_{M0}(1 + \alpha)$ ,  $\alpha$  being positive. Then, neglecting any error in  $C_D$ , the relative error  $\epsilon$  in the maximum force  $F$  (such that  $F = F_0(1 + \epsilon)$ ) is given by

$$\begin{aligned} \epsilon &= \frac{\alpha(2 + \alpha)}{1 + \frac{1}{2}\Phi^2} & \text{for } \Phi > \frac{1}{2} \\ \epsilon &= \alpha & \text{for } \Phi < \frac{1}{2} \end{aligned}$$

117. Table 7 gives the maximum values of  $\alpha$  as a function of the ratio  $C_D/C_M$  and  $N_K$  such that the calculated maximum force will differ by less than 10% from the force calculated using  $C_{M0}$ . For example, if  $C_D = 0.5$  is selected with an assumed  $C_M = C_{M0}$  value of 1.5, ( $C_D/C_M = \frac{1}{3}$ ) at  $N_K = 40$ , then the  $C_M$  value actually used could be up to 2.03 (= 1.5 (1 + 0.35)), without altering the relative error in the maximum force by more than 10%.

118. The maximum allowable error in  $C_D$  in inertia dominant conditions for less than 10% relative error in the maximum force at a particular depth may be estimated as follows.

119. Take the error in  $C_D$  as  $\beta$ , such that  $C_D = C_{D0}(1 + \beta)$ ,  $\beta$  being positive. Then, neglecting any error in  $C_M$  the relative error  $\epsilon$  in the maximum force  $F$  is given by

$$\epsilon = \frac{\beta + \gamma[1/(1 + \beta) - 1]}{1 + \gamma} \quad \text{for } \Phi > \frac{1}{2}$$

# DISCUSSION

Table 5. Values of  $F_D/F_I$

$N_K \backslash C_D/C_M$	$\frac{1}{8}$	$\frac{1}{4}$	$\frac{1}{2}$	$\frac{1}{2}$	$\frac{3}{4}$	1	2
5	0	0	0	0	0	0.01	1.55
11	0	0	0	0.12	0.90	1.98	9.44
15	0	0	0.01	0.65	2.10	4.12	18.00
20	0	0.01	0.41	1.53	4.12	7.71	32.30
25	0.01	0.30	0.93	2.71	6.72	12.30	50.80
40	0.81	1.55	3.15	7.71	18.00	32.30	131.00
70	3.52	5.79	10.70	24.70	56.10	100.00	402.00
100	7.71	12.30	22.30	50.80	115.00	205.00	820.00

Table 6. Values of  $F_{D \max}/F_{I \max}$

$N_K \backslash C_D/C_M$	$\frac{1}{8}$	$\frac{1}{4}$	$\frac{1}{2}$	$\frac{1}{2}$	$\frac{3}{4}$	1	2
5	0.10	0.13	0.17	0.25	0.38	0.51	1.01
11	0.22	0.28	0.37	0.56	0.84	1.11	2.23
15	0.30	0.38	0.51	0.76	1.14	1.52	3.04
20	0.41	0.51	0.68	1.01	1.52	2.03	4.05
25	0.51	0.63	0.84	1.27	1.90	2.53	5.07
40	0.81	1.01	1.35	2.03	3.04	4.05	8.11
70	1.42	1.77	2.36	3.55	5.32	7.09	14.18
100	2.03	2.53	3.38	5.07	7.60	10.13	20.26

Table 7. Maximum values of  $\alpha$

$N_X \backslash C_D/C_M$	$\frac{1}{8}$	$\frac{1}{4}$	$\frac{1}{2}$	$\frac{1}{2}$	$\frac{3}{4}$	1	2
5	0.10	0.10	0.10	0.10	0.10	0.10	0.23
11	0.10	0.10	0.10	0.11	0.17	0.26	0.76
15	0.10	0.10	0.10	0.15	0.27	0.42	1.19
20	0.10	0.10	0.13	0.23	0.42	0.66	1.77
25	0.10	0.12	0.18	0.32	0.59	0.91	2.37
40	0.17	0.23	0.35	0.66	1.19	1.77	4.23
70	0.38	0.54	0.83	1.48	2.52	3.61	8.03
100	0.66	0.91	1.38	2.37	3.92	5.49	11.86

Table 8. Maximum values of  $\beta$

$N_K \backslash C_D/C_M$	$\frac{1}{8}$	$\frac{1}{4}$	$\frac{1}{2}$	$\frac{1}{2}$	$\frac{3}{4}$	1	2
3	11.80	9.25	6.69	4.13	2.42	1.56	0.34
5	6.69	5.15	3.61	2.08	1.05	0.54	0.16
11	2.50	1.80	1.10	0.42	0.19	0.15	0.11
15	1.56	1.05	0.54	0.22	0.14	0.12	0.11
20	0.92	0.54	0.27	0.16	0.12	0.11	0.10
25	0.54	0.31	0.19	0.13	0.11	0.11	0.10
40	0.20	0.16	0.13	0.11	0.11	0.10	0.10

where

$$\gamma = 1/4\Phi^2 \quad \text{so } \gamma < 1$$

For  $\Phi < \frac{1}{2}$  ( $\gamma > 1$ )

$$\epsilon = \Phi(1+\beta) \left[ 1 + \frac{1}{4\Phi^2(1+\beta)} \right] - 1$$

120. Table 8 gives the maximum values of  $\beta$  as a function of the ratio  $C_D/C_M$  and  $N_K$ , such that the calculated maximum force will differ by less than 10% from the force calculated using  $C_{D0}$ . For example, if  $C_M=2.0$  is selected with an assumed  $C_D=C_{D0}$  value of 1.0 ( $C_D/C_M=\frac{1}{2}$ ), at  $N_K=11$ , then the  $C_D$  value used could be up to 1.42 ( $=1.0(1+0.42)$ ) without altering the relative error in the maximum force by more than 10%.